

Hsp27 knockdown using nucleotide-based therapies inhibit tumor growth and enhance chemotherapy in human bladder cancer cells

Masayuki Kamada,¹ Alan So,^{1,2}
Mototsugu Muramaki,¹ Palma Rocchi,¹
Elia Beraldi,¹ and Martin Gleave^{1,2}

¹The Prostate Centre, Vancouver General Hospital and

²Department of Urologic Sciences, University of British Columbia, Vancouver, British Columbia, Canada

Abstract

Heat shock protein 27 (Hsp27) is a cytoprotective chaperone that is phosphoactivated during cell stress that prevents aggregation and/or regulate activity and degradation of certain client proteins. Recent evidence suggests that Hsp27 may be involved in tumor progression and the development of treatment resistance in various tumors, including bladder cancer. The purpose of this study was to examine, both *in vitro* and *in vivo*, the effects of overexpression of Hsp27 and, correspondingly, the down-regulation of Hsp27 using small interfering (si) RNA and OGX-427, a second-generation antisense oligonucleotide targeting Hsp27. Hsp27 overexpression increased UMUC-3 cell growth and resistance to paclitaxel. Both OGX-427 and Hsp27 siRNA decreased Hsp27 protein and mRNA levels by >90% in a dose- and sequence-specific manner in human bladder cancer UMUC-3 cells. OGX-427 or Hsp27 siRNA treatment induced apoptosis and enhanced sensitivity to paclitaxel in UMUC-3 cells. *In vivo*, OGX-427 significantly inhibited tumor growth in mice, enhanced sensitivity to paclitaxel, and induced significantly higher levels of apoptosis compared with xenografts treated with control oligonucleotides. Collectively, these findings suggest that Hsp27 knockdown with OGX-427 and combined therapy with paclitaxel could be a novel strategy to inhibit the progression of bladder cancer. [Mol Cancer Ther 2007;6(1):299–308]

Introduction

Bladder cancer is the second most common malignancy of the genitourinary tract and the fifth leading cause of cancer-

related deaths of men in the western industrialized countries. Current treatments for superficial bladder cancer are of limited efficacy in preventing tumor recurrence and progression; after transurethral resection with or without intravesical chemotherapy, 50% to 70% of superficial bladder cancers will recur (1), and a significant proportion of patients with carcinoma *in situ* may develop invasive bladder cancer within 5 years (2). The prognosis of patients with invasive and/or metastatic bladder cancer is still extremely poor despite recent therapeutic advances (3). Cisplatin- and taxane-based combination chemotherapy is the mainstay of treatment for patients with advanced bladder cancer and is at least palliatively effective. However, the efficacy of combination chemotherapy is limited because of *de novo* drug resistance or the development of the cellular-resistant phenotype during treatment. Indeed, even in the era of intravesical therapy with Bacillus Calmette-Guerin and active systemic chemotherapy regimens, overall mortality rates for both bladder cancer and carcinoma *in situ* have remained constant in the U.S. (4). This underscores the need to identify mechanisms by which cancer cells inhibit the effects of chemotherapeutic agents, develop novel treatments, and consequently improve the survival of patients with advanced bladder cancer.

In addition to altered drug transport and metabolism, chemoresistance may also result from alterations in apoptotic "rheostat." Heat shock protein 27 (Hsp27) seems to play a crucial role in regulating the balance between cell death and cell survival, where its overexpression is associated with the suppression of apoptosis, increased cytoprotection, and resistance to treatment. Hsp27 belongs to a family of proteins that modulate a diverse range of homeostatic and pathogenic intracellular activities (5). Constitutively expressed Hsps are essential in cell homeostasis by acting as molecular chaperones to facilitate the transport, folding, and assembly of polypeptides. Hsp27 is phosphoactivated during cell stress to form oligomers that prevent aggregation and/or regulate activity and degradation of certain client proteins. Hsp27 expression is increased in a variety of malignancies, including prostate (6), breast (7), gastric (8), ovarian (9), and bladder cancers (10, 11). Furthermore, Hsp27 overexpression has been associated with multidrug resistance (12) and direct inhibition of apoptosis (13, 14) and is functionally linked to increased tumorigenicity and treatment resistance in breast (15) and colon (16) cancers.

Small molecule or antibody inhibitors that specifically target Hsp27 have not been reported. Antisense oligonucleotides (ASO) are powerful tools that specifically hybridize with complementary mRNA regions to form RNA/DNA

Received 7/18/06; revised 9/28/06; accepted 11/27/06.

The costs of publication of this article were defrayed in part by the payment of page charges. This article must therefore be hereby marked *advertisement* in accordance with 18 U.S.C. Section 1734 solely to indicate this fact.

Requests for reprints: Martin Gleave, The Prostate Centre, University of Columbia, Vancouver Hospital, 2660-Oak Street, Vancouver, BC, Canada V6H-3Z6. Phone: 604-875-5003; Fax: 604-875-5604. E-mail: m.gleave@ubc.ca

Copyright © 2007 American Association for Cancer Research.

doi:10.1158/1535-7163.MCT-06-0417

duplexes to inhibit target gene expression in a sequence-specific manner. Several ASOs targeting genes involved in neoplastic progression have been evaluated as potential therapeutic agents (17, 18). In fact, the combined use of ASO with other compounds, such as chemotherapeutic agents, has shown synergistic antineoplastic effects in several tumor models (18, 19). OGX-427 (OncoGenex, Vancouver, BC, Canada) is a second-generation ASO, generated using the 2'-O-(2-methoxy) ethyl (2'-MOE) backbone, that targets Hsp27 mRNA. In this study, we functionally analyzed the role of Hsp27 in bladder cancer cell survival using the UMUC-3 cell line both *in vitro* and *in vivo* and identified a role for Hsp27 in promoting UMUC-3 cell growth and chemoresistance. We then tested the effect of OGX-427 on the growth of Hsp27-expressing human UMUC-3 bladder cancer cells and found that this drug candidate potently suppresses Hsp27 levels, decreases cell growth rates through the induction of apoptosis, and chemosensitizes UMUC-3 cells both *in vitro* and *in vivo*.

Materials and Methods

Cells and Reagents

UMUC-3 cells were purchased from the American Type Culture Collection (Manassas, VA) and maintained in DMEM supplemented with 10% fetal bovine serum. UMUC-3 cells are human transitional carcinoma cells that are high grade and highly invasive (20). Paclitaxel was purchased from Biolyse Pharma (St. Catharines, ON, Canada). Stock solutions of paclitaxel were prepared with PBS to the required concentrations before each *in vitro* experiment. Dr. Helen M. Burt (Pharmaceutical Sciences, University of British Columbia, Vancouver, BC, Canada) generously supplied polymeric micellar paclitaxel used for *in vivo* studies.

Lentiviral Infection of Hsp27 into UMUC-3 cells

Human Hsp27 cDNA was subcloned into the lentiviral vector pHR'-CMV-EGFP at the *Bam*HI and *Xho*I sites. Two vectors were created for study: pHR'-CMV-Hsp27 and pHR'-CMV (empty vector). Clone identity was verified using restriction digestion analysis and plasmid DNA sequencing. Infectious lentivirus was generated by cotransfection of 1.5×10^6 293T cells with target plasmids with pCMV Δ R8.2 (carries the sequence necessary for viral assembly of lentivirus) and pMD.G that express the vesicular stomatitis virus envelop glycoprotein G(VSV-G) pseudotype as described previously (21, 22). The 293T cells were transfected with Hsp27-expressing, enhanced green fluorescent protein-expressing, or empty lentiviral vector (10 μ g of each) using the calcium phosphate precipitation method (Promega Protection Mammalian Transfection Systems, Promega, Madison, WI). 293T cells were transfected for 12 to 15 h, after which fresh medium was added for 24 h. Following this, the virus-containing media were collected and filtered through a 0.45- μ m filter. Early-passage UMUC-3 cells (passage 30) were plated in 10-cm plates, and competent retrovirus was added to 30 to

40 multiplicity of infection. The cells were passaged and harvested for fluorescence microscopy to verify green fluorescent protein expression. The whole cell lysates were collected to ensure the expression of Hsp27 by Western blotting. Images were captured using a Zeiss Axioplan II fluorescence microscope at $\times 63$ magnification followed by analysis with an imaging software (Northern Eclipse, Empix Imaging, Inc., Mississauga, ON, Canada). Analysis of focal localization was also done with Northern Eclipse and Adobe Photoshop 5.5 software.

OGX-427 and siRNA

2'-O-(2-methoxyethyl) ASO, OGX-427, was obtained from OncoGenex. The sequence of OGX-427 corresponds to the human Hsp27 translation initiation site (5'-GGGACGGG-CGCTCGGTCAT-3'). A mismatch oligodeoxynucleotide (ODN; 5'-CAGCAGCAGAGTATTTATCAT-3') was used as a control. The sequence of Hsp27 small interfering (si) RNA corresponds to the human Hsp27 site (5'-GUCUCAUCGGAUUUUGCAGC-3'; Dharmacon, Lafayette, CO). A scrambled siRNA (5'-CAGCGCUGACAACAGUUUCAU-3') was used as a control for RNA interference experiments.

Treatment of Cells with OGX-427 and siRNA

Cells were plated at the density of 4,000 cells per 1.9 cm² and treated 1 day later for 1 or 2 days with ASO or siRNA, respectively. OligofectAMINE (Invitrogen-Life Technologies, Inc., Carlsbad, CA) was used as a transfection agent for both ODN or siRNA uptake into the cells. UMUC-3 cells were treated with various concentrations of ODN or siRNA after a preincubation for 20 min with 3 mg/mL OligofectAMINE in serum-free OPTI-MEM (Invitrogen-Life Technologies, Inc.).

Northern Blot Analysis

Total RNA was isolated from cultured UMUC-3 cells and tumor tissues using the TRIzol method (Invitrogen, Carlsbad, CA). Electrophoresis, hybridization, and washing conditions were carried out as reported previously (18, 23). Human Hsp27 cDNA probe was obtained from StressGen (Victoria, BC, Canada). The density of bands for Hsp27 was normalized against that of glyceraldehyde-3-phosphate dehydrogenase by densitometric analysis (Scion Image, Scion Corporation, Frederick, MD). Each assay was done in triplicate.

Western Blot Analysis

Samples containing equal amounts of protein (10-40 μ g) from lysates of cultured UMUC-3 cells underwent electrophoresis on a SDS-polyacrylamide gel and were then transferred to a nitrocellulose filter. Filters were blocked in PBS containing 5% nonfat milk powder at 4°C overnight and then incubated for 1 h with a 1:5,000 diluted antihuman Hsp27 rabbit polyclonal antibody (StressGen), caspase-3 rabbit polyclonal antibody (New England BioLabs, Inc., Mississauga, ON, Canada), poly(ADP-ribose) polymerase rabbit polyclonal antibody (Cell Signaling Technology Inc., Beverly, MA) and antivinculin mouse monoclonal antibody (Sigma, St. Louis, MO). Filters were then incubated for 30 min with 1:5,000 diluted horseradish peroxidase-conjugate antirabbit or mouse monoclonal antibody (Santa Cruz Biotechnology, Inc., Santa Cruz, CA). Specific proteins

were detected using an enhanced chemiluminescence Western blotting analysis system (Amersham Life Science, Arlington Heights, IL). The density of bands for Hsp27 was normalized against that of vinculin by densitometric analysis (Scion Image, Scion Corporation). Each assay was done in triplicate.

***In vitro* Cell Growth Assays**

To examine the effect of Hsp27 overexpression on cell growth, 2×10^3 cells were seeded in 96-well microtiter plates, and cell viability was determined by 3-(4,5-dimethylthiazol-2-yl)-2,5-diphenyltetrazolium bromide (MTT) assay at 24, 48, and 72 h as described previously (24). Briefly, the MTT assay is a quantitative method of determining the number of live cells to evaluate rates of cell growth or death. To assess chemosensitivity, cells were incubated in media plus paclitaxel at various concentrations for 48 h after 5×10^3 cells were plated. To determine the effect of down-regulation of Hsp27 in parental UMUC-3 cells, which constitutively express Hsp27, UMUC-3 cells were transfected with OGX-427 or control ODN. All cells were seeded 96-well microtiter plates. After 24 h, cells were then treated once daily with indicated concentration of ODN for 2 days. After 48 h, cell viability was measured by MTT assay.

To assess the effect of the combination treatment of OGX-427 plus paclitaxel, cells were transfected with 50 nmol/L OGX-427 or 50 nmol/L control ODN as described above and then treated with indicated concentrations of paclitaxel for 2 days. Cell viability was then determined by MTT assay.

Flow Cytometric Analysis

Flow cytometric analysis of propidium iodide-stained nuclei was done to quantify apoptotic rates using the sub-G₀-G₁ cell fraction, as described previously (18, 23). Briefly, UMUC-3 cells were plated and then transfected with ODN (with or without paclitaxel) as described above. The cells were trypsinized at 1 day after last treatment (with or without 25 nmol/L paclitaxel) and analyzed for relative DNA content on a dual laser flow cytometer (Beckman Coulter Epics Elite; Beckman, Inc., Miami, FL). Each assay was done in triplicate.

Assessment of Growth of UMUC-3 Tumor *In vivo*

Approximately 5×10^6 UMUC-3 cells were inoculated s.c. in the flank region of 8-week-old male athymic nude mice (Harlan Sprague-Dawley, Inc., Indianapolis, IN) via a 27-gauge needle under halothane anesthesia. Each experimental group consisted of 10 mice. When UMUC-3 tumors reached 100 mm³, mice were randomly selected for treatment with OGX-427 or control ODN alone. To assess the effects of OGX-427 monotherapy, 12 mg/kg OGX-427 or control ODN was injected i.p. once daily for 7 days followed by three weekly treatments thereafter. To assess whether OGX-427 enhances paclitaxel activity *in vivo*, when UMUC-3 tumors reached 500 mm³, mice were randomly selected for treatment with paclitaxel plus OGX-427 or control ODN. In combination treatment groups, 0.5 mg/kg paclitaxel was administered i.v. thrice per week from days 28 to 35 and from days 42 to 49. Tumor volume measure-

ments were done once weekly and calculated by the formula length \times width \times depth \times 0.5236 (25). Data points were expressed as average tumor volume levels \pm SE. All animal procedures were done according to the guidelines of the Canadian Council on Animal Care and with appropriate institutional certification.

TUNEL Apoptosis Assay

For terminal nucleotidyl transferase-mediated nick end labeling (TUNEL) assay, tissue sections (5 μ m thick) of formalin-fixed, paraffin-embedded specimens were deparaffinized in xylene, rehydrated in graded alcohol, and transferred to PBS. The slides were rinsed twice with distilled water and treated with a 1:500 proteinase K solution (20 μ g/mL) for 15 min, and endogenous peroxidase was blocked with 3% hydrogen peroxide in PBS for 12 min. The samples were washed thrice with distilled water and incubated for 10 min at room temperature with terminal deoxynucleotidyl transferase buffer. Excess terminal deoxynucleotidyl transferase buffer was drained, and the samples were incubated for 18 h at 4°C with terminal transferase and biotin-16-dUTP. The samples were then rinsed four times with TB buffer and incubated for 30 min at 37°C with a 1:400 dilution of peroxidase-conjugated streptavidin. The slides were rinsed with PBS and incubated for 5 min with diaminobenzidine (Invitrogen-Life Technologies, Inc.). The sections were then washed thrice with PBS, counterstained with Gill's hematoxylin (Biogenex, San Ramon, CA), and again washed thrice with PBS. The slides were mounted with a Universal Mount (Research Genetics).

Quantification of Cell Proliferation and Apoptosis

Effects of various treatments on tumor cell proliferation and apoptosis were determined by immunohistochemistry staining of tissue sections with anti-proliferating cell nuclear antigen antibodies and the TUNEL assay. The tissue was recorded using a cooled CCD Optotronics Tec 470 camera (Optotronics Engineering, Goleta, CA) linked to a computer and digital printer (Sony Corporation, Shinagawa, Tokyo, Japan). The density of proliferative cells and apoptotic cells was expressed as an average number of the five highest areas identified within a single 400 \times field.

Statistical Analysis

All results are expressed as the mean \pm SD, and the significance of differences were by Student's *t* test or ANOVA-repeated measurement (SPSS 11.0 for Windows, Tokyo, Japan). *P* values <0.05 and <0.01 were considered significant by Student's *t* test and *P* < 0.01 by ANOVA-repeated measurement.

Results

Hsp27 Overexpression Increases Cell Growth and Chemoresistance in UMUC-3 Cells

Western blot analysis confirmed high expression levels of Hsp27 in Hsp27-transfected cells (UMUC-3-hsp27), compared with empty vector-transfected cells (UMUC-3-mock) and parental controls (UMUC-3; data not shown).

Cell growth rates were higher in UMUC-3-hsp27 cells compared with parental cells and vector-only-transfected cells ($P < 0.01$). Moreover, Hsp27 overexpression increased resistance to paclitaxel; the IC_{50} of UMUC-3-Hsp27 cells was >50-fold higher than that in UMUC-3 or UMUC-3-mock cells ($P < 0.01$).

Sequence-Specific and Dose-Dependent Inhibition of Hsp27 Expression by OGX-427 and siRNA

OGX-427 significantly down-regulated Hsp27 in a dose-dependent fashion. As shown in Fig. 1A and B, OGX-427 treatment significantly reduced Hsp27 mRNA levels by up to 80% in a dose-dependent manner, whereas Hsp27 protein levels, as shown in Fig. 1C and D, was reduced by >95% after OGX-427 treatment. Similarly, Hsp27 siRNA inhibited Hsp27 mRNA and protein levels in dose-dependent manner (Fig. 2A-D).

OGX-427-induced Hsp27 Knockdown Increases Apoptotic Rates in UMUC-3 Cells

Hsp27 has been reported to interact with caspase-3, thereby inhibiting caspase-3 activation (26). Cells treated with OGX-427 expressed significantly higher amounts of cleaved caspase-3 and poly(ADP-ribose) polymerase products compared with cells treated with control ODN (Fig. 3A). In addition, the induction of apoptosis by Hsp27 ASO was also clearly shown using flow cytometry. The apoptotic sub- G_0 - G_1 fraction was significantly higher after

Hsp27 knockdown using 50 nmol/L OGX-427 compared with 50 nmol/L control ODN (39.5% versus 11.2%, Fig. 3B and C). Furthermore, combination treatment using OGX-427 plus paclitaxel significantly increased the sub- G_0 - G_1 fraction over that of paclitaxel plus control ODN (68.4% versus 42.2%, Fig. 3B and C).

OGX-427 Inhibits UMUC-3 Cell Growth and Enhances Paclitaxel Sensitivity *In vitro*

To determine whether the reduction of Hsp27 expression affects UMUC-3 cell growth or paclitaxel chemosensitivity *in vitro*, cells were treated for 2 days with 50 nmol/L Hsp27 ASO or control ODN, with or without increasing concentrations of paclitaxel. OGX-427 treatment reduces UMUC-3 cell growth in a dose-dependent manner (Fig. 4A) and significantly chemosensitizes UMUC-3 cells to paclitaxel (Fig. 4A), reducing the IC_{50} of paclitaxel in UMUC-3 cells >2-fold (Fig. 4B, $P < 0.01$). Collectively, these data suggest that Hsp27 knockdown inhibits cell growth and increases chemosensitivity by increasing the rate of apoptosis, in part by preventing Hsp27-regulated inhibition of caspase-3 activation.

Effects of OGX-427 Treatment on UMUC-3 Xenograft Growth

We next evaluated the effects of Hsp27 ASO treatment on the growth of UMUC-3 tumors *in vivo* (Fig. 4C). Male nude mice bearing UMUC-3 tumors (200 mm^3) were randomly

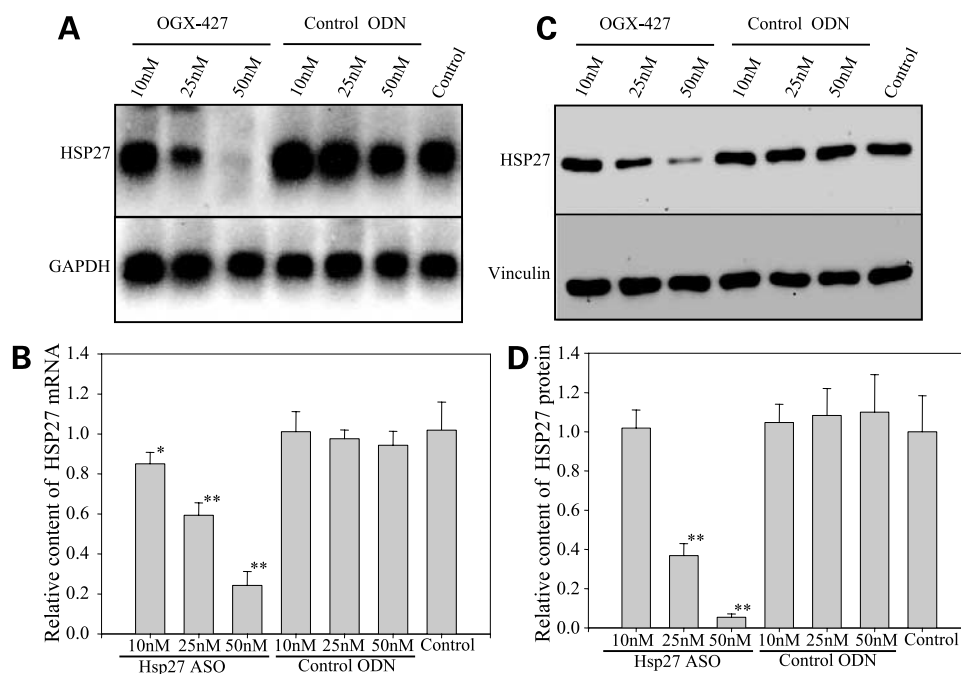
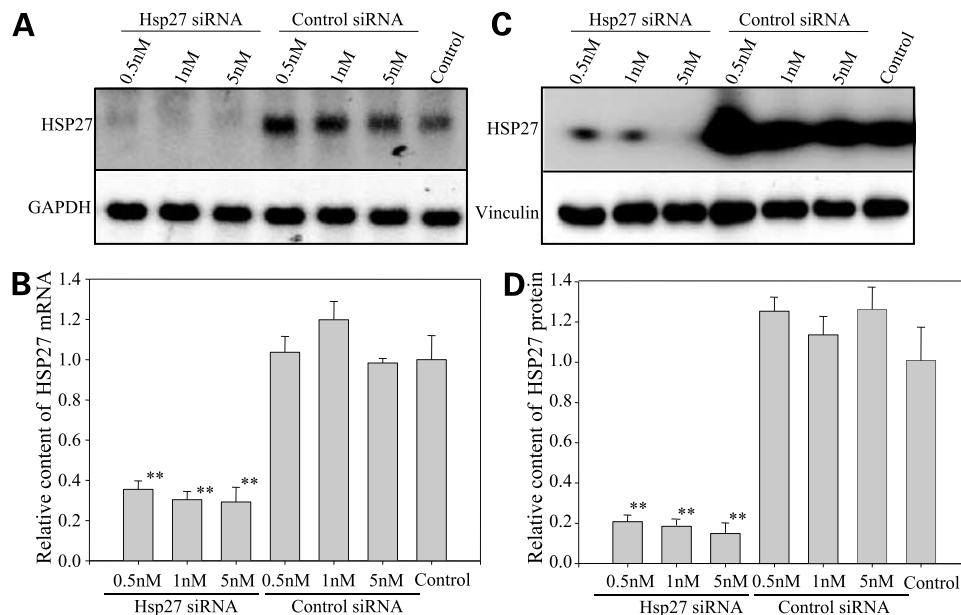


Figure 1. Sequence-specific and dose-dependent suppression of Hsp27 mRNA and protein expression levels by OGX-427 in UMUC-3 cells. **A**, UMUC-3 cells were treated with 10, 25, and 50 nmol/L OGX-427 or control ODN for 2 d. One day after treatment, total cellular RNA was extracted, and Hsp27 and glyceraldehyde-3-phosphate dehydrogenase (GAPDH) mRNA expression were analyzed by Northern blotting. **Control**, cells treated with OligofectAMINE only. **B**, quantitative analysis of Hsp27 mRNA levels from **A** after normalization to GAPDH by densitometric analysis. **C**, UMUC-3 cells were treated with various concentrations of OGX-427 and control ODN for 2 d. Two days after treatment, cellular proteins were extracted from cultured cells, and Hsp27 and vinculin protein levels were analyzed by Western blotting. **D**, quantitative analysis of Hsp27 protein levels from **C** after normalization to vinculin by densitometric analysis. *, $P < 0.05$; **, $P < 0.01$ differ from control ODN by Student's *t* test.

Figure 2. Sequence-specific and dose-dependent suppression of Hsp27 mRNA and protein expression level by Hsp27 siRNA in UMUC-3 cells. **A**, UMUC-3 cells were treated with 0.5, 1, and 5 nmol/L Hsp27 siRNA or control siRNA for 1 d. One day after treatment, total cellular RNA was extracted, and Hsp27 and GAPDH mRNA expression were analyzed by Northern blotting. **B**, quantitative analysis of Hsp27 mRNA levels from **A** after normalization to GAPDH by densitometric analysis. **C**, UMUC-3 cells were treated with 0.5, 1, and 5 nmol/L Hsp27 siRNA or control siRNA for 2 d. Total cellular protein was extracted, and Hsp27 and GAPDH expression levels were analyzed by Western blotting. **D**, quantitative analysis of Hsp27 protein levels from **C** after normalization to vinculin by densitometric analysis. *, $P < 0.01$, differs from control ODN by Student's *t* test.



selected for 12 mg/kg Hsp27 ASO versus control ODN and ODN by i.p. injection. From days 7 to 14 and 21 to 28, 0.5 mg micellar paclitaxel was administered i.v. once daily. Mean UMUC-3 tumor volume was similar in all mice before treatment (Fig. 4C). Growth differences began to emerge after 2 weeks of ODN therapy (Fig. 4C); mice treated with OGX-427 monotherapy had significant growth inhibition compared with control ODN. These differences continued to increase to day 42, when OGX-427-treated xenografts were half the size of control ODN-treated tumors.

Xenografts treated with combination OGX-427 plus paclitaxel had significant growth inhibition compared with tumors treated with paclitaxel plus control ODN (Fig. 4D). These differences continued to increase after the second treatment of paclitaxel (day 49) until the end of the *in vivo* experiment. These results further illustrate the additive effects of combination therapy of OGX-427 and paclitaxel and corroborate the *in vitro* results.

To quantify the level of Hsp27 knockdown induced by OGX-427, xenografts treated with OGX-427 or control ODN, plus or minus paclitaxel, were analyzed by Northern blotting (Fig. 5A). Hsp27 mRNA expression in OGX-427-treated tumors was significantly down-regulated compared with that of control ODN-treated tumors (Fig. 5B). TUNEL assay was done to quantify the difference in apoptotic cells in UMUC-3 tumor tissues. Xenografts treated with OGX-427 had significant higher amounts of apoptosis compared with tumors treated with control ODN (Fig. 5Ci and D).

Discussion

Alterations in the apoptotic rheostat of cancer cells contribute to the development of chemoresistance. Defining

mechanisms of action of apoptotic-regulatory proteins associated with treatment resistance may identify strategies to selectively manipulate the sensitivity of cancer cells to therapy. Recent evidence suggests that Hsp27 plays an integral role in treatment resistance in many malignancies. Hsps are a family of highly conserved proteins in which expression is induced by cell stressors, such as hyperthermia, oxidative stress, and cytotoxic drugs (27). Hsps have attracted attention as new therapeutic targets for cancer, especially since the discovery and characterization of geldanamycin as an inhibitor of Hsp90 (28) and the targeting of clusterin (24, 29, 30) in which the product has Hsp-like function. Hsp27 is an ATP-independent chaperone that prevents the aggregation or regulate activity and degradation of certain client proteins.

Hsp27 interacts with key apoptosis-associated proteins and functions to inhibit cell death by a variety of mechanisms. Hsp27 prevents the formation of the apoptosome by either preventing the release of mitochondrial cytochrome *c* or directly sequestering cytochrome *c* in the cytosol after mitochondrial release (31). Hsp27 also directly interacts with and inhibits caspase-3 activation (26). Hsp27 can interfere with the extrinsic cell death pathway by inhibiting Daxx, a mediator of Fas-induced caspase-independent apoptosis (32). Furthermore, Hsp27 has been shown to inhibit apoptosis by decreasing the reactive oxygen species within cells by increasing glutathione and reducing the toxic effect of oxidized proteins (33). In addition, Hsp27 acts early during cell stress to stabilize and accelerate the recovery of actin filaments, thus preventing the disruption of the cytoskeleton (34). Hsp27 is also involved in the regulation of the serine/threonine kinase AKT (protein kinase B), an important signaling molecule for cell survival and proliferation

304 *OGX-427 Down-regulation of Hsp27 in Bladder Cancer*

downstream of growth factor stimulation (35). Hsp27 can exert its antiapoptotic effects through the enhancement of nuclear factor- κ B activity, by facilitating proteasomal degradation of its main inhibitor I- κ B (36). Finally, we

recently reported that Hsp27 interacts with and increases signal transducers and activators of transcription 3 levels and activity, a relevant transcription factor in many cancers, identifying yet another cytoprotective mechanism

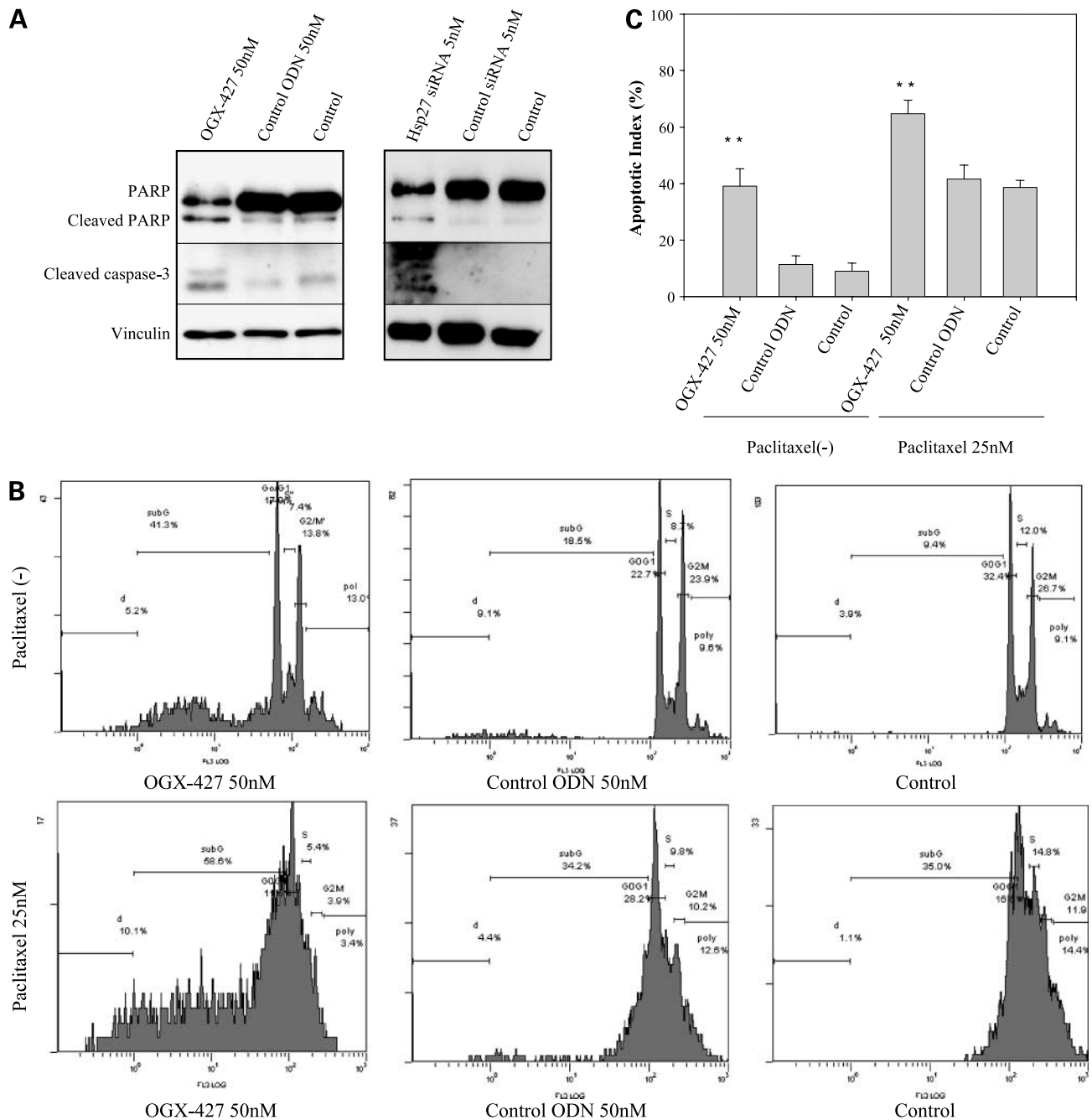


Figure 3. Hsp27 knockdown induces apoptosis. **A**, poly(ADP-ribose) polymerase (PARP) and caspase-3 expression after treatment with OGX-427 or Hsp27 siRNA. UMUC-3 cells were treated daily with 50 nmol/L OGX-427 or control ODN, and Hsp27 siRNA or control siRNA for 1 or 2 d, respectively. After 48 h of incubation, cells were harvested, and protein was extracted for detection of poly(ADP-ribose) polymerase and cleaved caspase-3. Poly(ADP-ribose) polymerase antibody, cleaved caspase-3 antibody, and vinculin antibody were used for Western blotting. Vinculin was used as a positive control. **B**, flow cytometry after treatment with OGX-427. UMUC-3 cells were treated with 50 nmol/L OGX-427 or control ODN daily for 2 d. After 24 h of incubation with medium \pm 25 nmol/L paclitaxel, flow cytometry was used to quantify the percentage of cells in each phase which is shown in the order of sub-G₀-G₁, G₀-G₁, S, and G₂ + M. After OGX-427 \pm paclitaxel treatment, the percentage of cells in sub-G₀-G₁ were counted. **C**, plot of the mean sub-G₀-G₁ fraction from three separate flow samples. **, $P < 0.01$ (Student's t test).

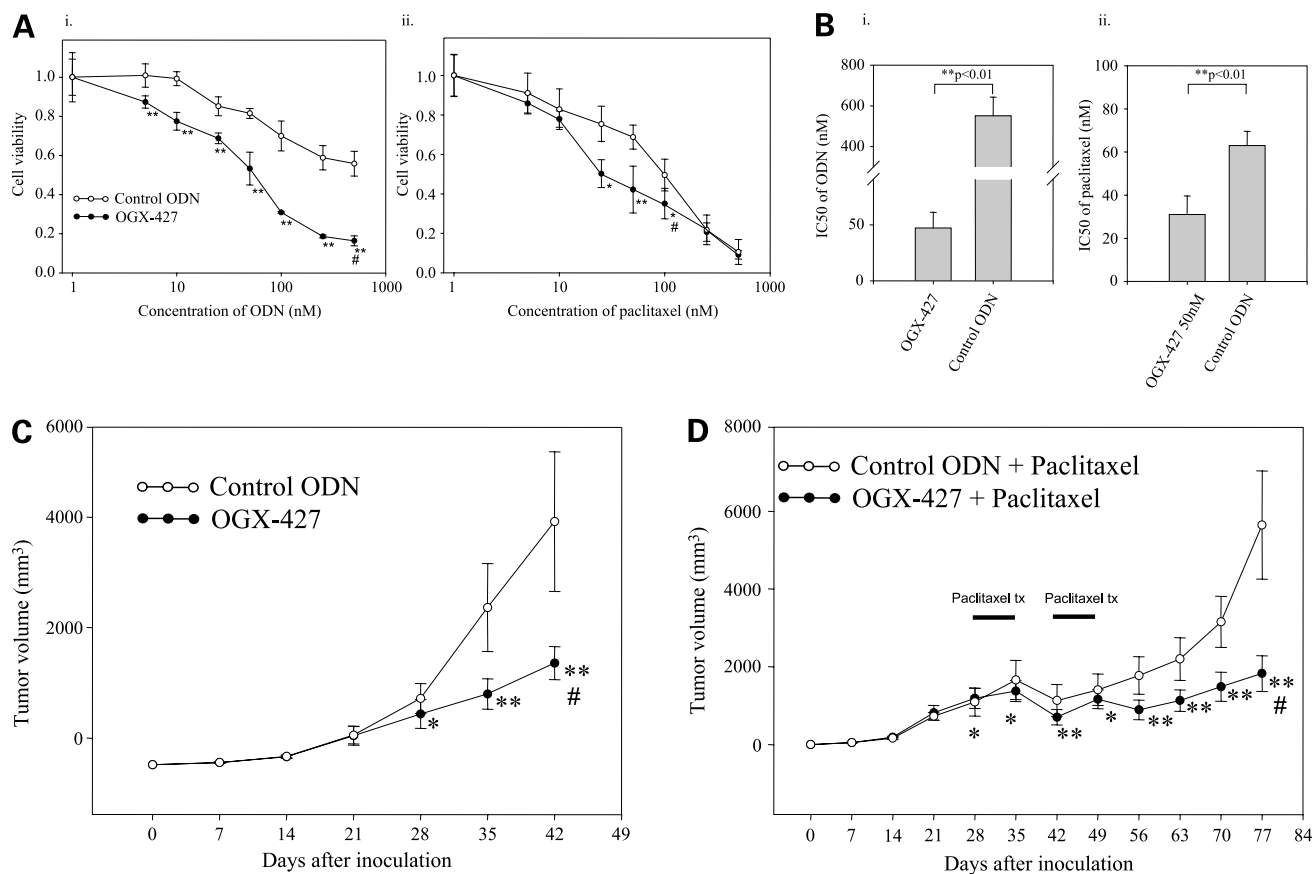


Figure 4. Cytotoxic effect of OGX-427 treatment or combined treatment with OGX-427 and paclitaxel. **A**, UMUC-3 cells were treated with various concentration of OGX-427 or control ODN for 2 d \pm paclitaxel. **i**, cells treated with increasing concentrations of ODN alone; cell viability determined by MTT assay after 48 h of treatment. **ii**, cells treated with ODN and paclitaxel; cells were initially treated with 50 nmol/L of ODN (either OGX-427 or control ODN). Chemotherapy of increasing concentrations was added after 2 d of treatment with respective ODN. After 24 h of incubation, cell viability was determined by MTT assay. **B**, IC₅₀ was calculated from cell viability plots. The difference in each IC₅₀ (**i**, ODN monotherapy; and **ii**, combination therapy of ODN + paclitaxel) was analyzed by Student's *t* test. **, $P < 0.01$; #, $P < 0.01$ (ANOVA-repeated measurement). **C**, effects of OGX-427 monotherapy *in vivo*. When tumor volume was ~ 100 mm³ (day 14), OGX-427 treatment was started. After 1 wk of an induction daily dose of 12 mg/kg/mouse OGX-427 or control ODN given *i.p.*, mice were injected with the same dose thrice per week. Tumors were measured weekly. **D**, effects of combination therapy *in vivo*. Combination treatment was started when tumor volume reached ~ 500 mm³ (day 21). After 1 wk of a daily induction dose of either OGX-427 or control ODN at 12 mg/kg/mouse, mice were injected with similar doses thrice a week. Two cycles of *i.v.* paclitaxel treatment were given on days 28 to 35 and 42 to 49 at 0.5 kg/mg/mouse. *, $P < 0.05$, ** $P < 0.01$ (Student's *t* test); #, $P < 0.01$ (ANOVA-repeated measurement).

mediated by Hsp27 (37). Thus, Hsp27 is an attractive therapeutic target because its inhibition would affect multiple different pathways implicated in cancer cell survival and resistance as opposed to targeting a single pathway.

Hsp27 is highly expressed in many human tumors, including prostate, breast, ovarian, gastric, and bladder cancers (6, 8, 9, 38). Although Hsp27 is expressed at low levels in normal bladder epithelial cells (39), Hsp27 expression is induced in transitional cells after exposure to heat and carcinogens (40). Accordingly, Kassem et al. have shown, using an elegant cDNA microarray analysis with quantitative reverse transcription-PCR confirmation, that high levels of Hsp27 are associated with radioresistance, and more importantly, that low Hsp27 expression may be a marker to predict bladder tumors that are sensitive to radiotherapy (41). Furthermore, Lebre's

analysis of 42 patients with superficial bladder cancer showed that Hsp27 was highly expressed (*i.e.*, >50% of cells) in 83% of tumors (11). In our series of 11 carcinoma *in situ* specimens obtained from transurethral resection, a high level of Hsp27 was expressed in all specimens relative to normal controls (data not shown). However, to our knowledge, there have been no studies analyzing the functional significance of Hsp27 expression in bladder cancer.

In this study, we identify, for the first time, the functional role of Hsp27 in bladder cancer growth and treatment resistance. Hsp27 overexpression in UMUC-3 cells accelerates cell growth and increases resistance against paclitaxel, whereas Hsp27 knockdown by OGX-427 or Hsp27 siRNA *in vitro* enhances the induction of apoptosis and chemosensitizes cells to paclitaxel. *In vivo*, OGX-427 monotherapy significantly inhibited tumor growth, and

306 **OGX-427 Down-regulation of Hsp27 in Bladder Cancer**

the combination therapy of OGX-427 with paclitaxel significantly inhibited tumor growth and enhanced apoptosis compared with tumors treated with paclitaxel plus control ODN. Because UMUC-3 cells have mutant p53, OGX-427 likely induces p53-independent apoptotic triggers (42). Collectively, these findings show that Hsp27 helps mediate bladder cancer progression and development of treatment resistance to cytotoxic chemotherapy. The response to OGX-427 in UMUC-3 cells are similar to our previous reports of Hsp27 knockdown in LNCaP and PC-3 prostate cancer cell lines (18, 37). In these studies, OGX-427 enhanced the *in vivo* effects of castration-induced regression to delay androgen-independent LNCaP and PC-3 tumor growth and also enhances chemotherapy *in vivo*, emphasizing the additive role this ASO has in combination therapy regimes.

Most cases of locally advanced or metastatic bladder cancer initially respond to combination chemotherapy; however, the development of an acquired resistant phenotype frequently occurs with the progression of the disease (2). Recently, several investigators have shown that over-expression of antiapoptotic genes in bladder cancer cells, such as clusterin (43), Bcl-2 (44), or mutant-type p53 (45), helps mediate drug resistance through the inhibition of apoptosis induced by chemotherapeutic agents, suggesting that the approach of enhancing chemosensitivity by decreasing the expression of antiapoptotic genes may be a rational strategy for patients with advanced bladder cancer. Furthermore, recent studies provide preclinical proof of principle that targeting antiapoptotic genes using ASO can enhance apoptosis induced by conventional cytotoxic chemotherapy (46). Knockdown of Hsp27 using

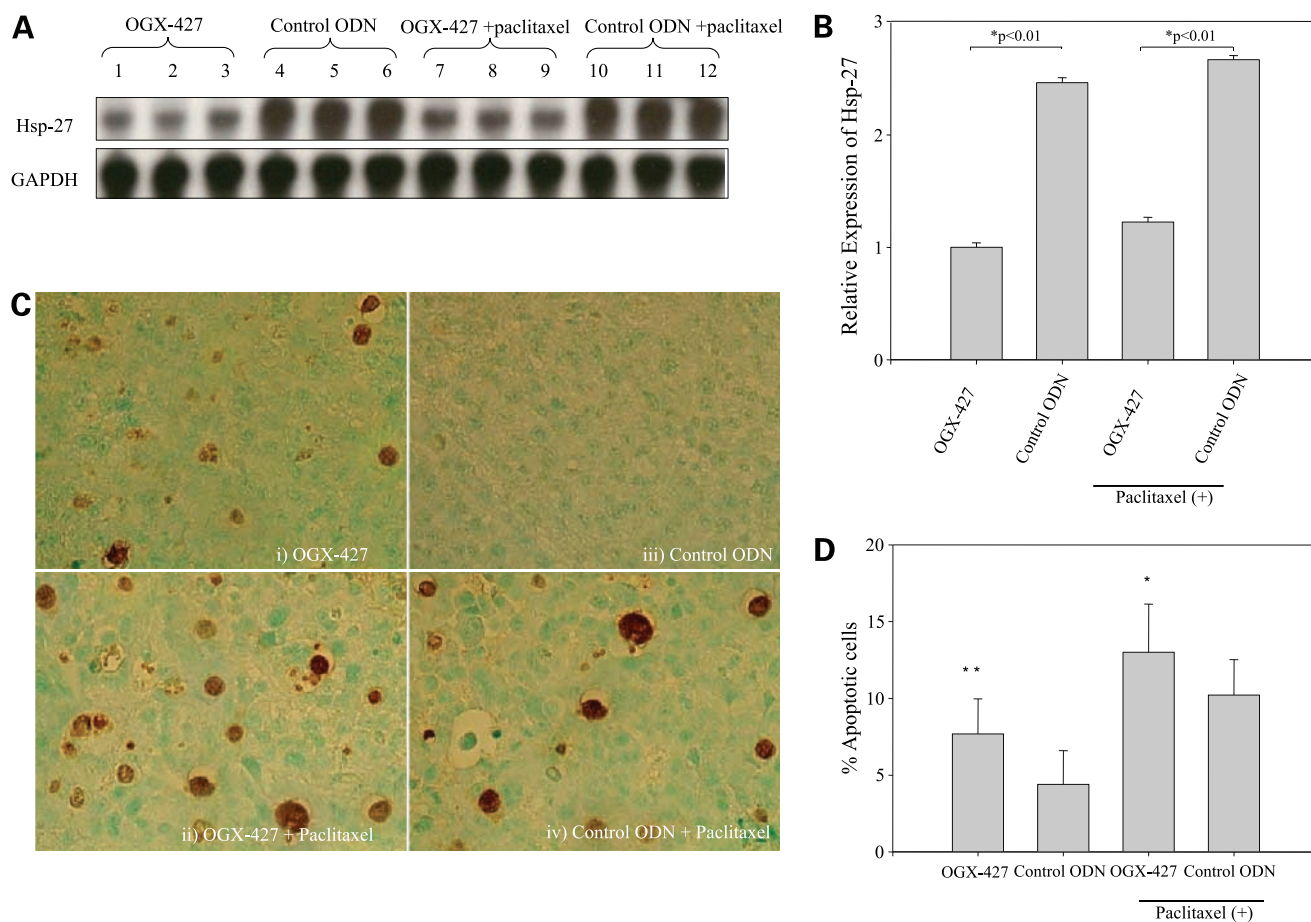


Figure 5. Effect of OGX-427 ip treatments on Hsp27 expression in UMUC-3 xenografts. **A**, mice were sacrificed after treatment with OGX-427 or control ODN and \pm i.v. paclitaxel. Total RNA was extracted from tumor tissue, and then Hsp27 and GAPDH were analyzed by Northern blotting. *Lanes 1 to 3*, OGX-427 administered to UMUC-3 tumors in mice; *lanes 4 to 6*, control ODN administered to UMUC-3 tumors in mice; *lanes 7 to 9*, OGX-427 Hsp27 + paclitaxel administered to UMUC-3 tumors in mice; *lanes 10 to 12*, control ODN plus paclitaxel administered to UMUC-3 tumors in mice. **B**, quantitative analysis of Hsp27 levels after normalization to GAPDH mRNA levels were determined by densitometric analysis. **C**, UMUC-3 tumors were harvested from each treatment group for detection of apoptosis using TUNEL staining. Sections of paraffin-embedded UMUC-3 tumors were stained with digoxigenin-dUTP antibody to detect apoptotic cells and imaged at 40 \times magnification. *i*, UMUC-3 tumor after treatment with OGX-427; *ii*, UMUC-3 tumor after treatment with control ODN; *iii*, UMUC-3 tumor after treatment with OGX-427 plus paclitaxel; *iv*, UMUC-3 tumor after treatment with control ODN plus paclitaxel. **D**, after TUNEL staining, the number of apoptotic cells was counted and expressed as a proportion of the total number of cells in each microscope field at a magnification \times 400. Ten fields were examined. Columns, means; bars, SD. *, $P < 0.05$, ** $P < 0.01$ (Student's *t* test).

ASO like OGX-427 may also be a rational approach in the treatment of superficial bladder cancer, where the main goal is the prevention of tumor recurrence and progression to muscle-invasive disease. Unfortunately, current treatment regimens have limited success in achieving these goals. The accessibility of the bladder mucosa and the low systemic absorption through the bladder wall make intravesical therapy an excellent route of administration of ASO. Although no studies have yet been reported that assess pharmacokinetic and pharmacodynamic activity of ASO after intravesical delivery in humans, preclinical studies would suggest that ASO are taken up by urothelium (47, 48). Interestingly, the only approved clinical indication for an ASO is for intravitreal injection of cytomegalovirus-induced retinitis in human immunodeficiency virus, illustrating the potential clinical utility of local instillation for this class of therapeutics (49).

In summary, the present study suggests that the expression of Hsp27 helps mediate bladder cancer progression by inhibiting apoptotic cell death induced by cytotoxic chemotherapy. OGX-427 down-regulation of Hsp27 in UMUC-3 cells inhibits growth, induces apoptosis, and chemosensitizes cells to chemotherapy. These results provide preclinical proof of principle for the use of this novel therapeutic in the treatment of bladder cancer.

References

- Wolf H, Melsen F, Pedersen SE, Nielsen KT. Natural history of carcinoma *in situ* of the urinary bladder. *Scand J Urol Nephrol Suppl* 1994;157:147–51.
- Malmstrom PU, Busch C, Norlen BJ. Recurrence, progression and survival in bladder cancer. A retrospective analysis of 232 patients with greater than or equal to 5-year follow-up. *Scand J Urol Nephrol* 1987;21:185–95.
- Thurman SA, DeWeese TL. Multimodality therapy for the treatment of muscle-invasive bladder cancer. *Semin Urol Oncol* 2000;18:313–22.
- American Cancer Society. Cancer facts and figures. American Cancer Society 2006.
- Raine CS, Wu E, Ivanyi J, Katz D, Brosnan CF. Multiple sclerosis: a protective or a pathogenic role for heat shock protein 60 in the central nervous system? *Lab Invest* 1996;75:109–23.
- Cornford PA, Dodson AR, Parsons KF, et al. Heat shock protein expression independently predicts clinical outcome in prostate cancer. *Cancer Res* 2000;60:7099–105.
- Love S, King RJ. A 27 kDa heat shock protein that has anomalous prognostic powers in early and advanced breast cancer. *Br J Cancer* 1994;69:743–8.
- Ehrenfried JA, Herron BE, Townsend CM Jr., Evers BM. Heat shock proteins are differentially expressed in human gastrointestinal cancers. *Surg Oncol* 1995;4:197–203.
- Langdon SP, Rabiasz GJ, Hirst GL, et al. Expression of the heat shock protein Hsp27 in human ovarian cancer. *Clin Cancer Res* 1995;1:1603–9.
- Takashi M, Katsuno S, Sakata T, Ohshima S, Kato K. Different concentrations of two small stress proteins, α B crystallin and Hsp27 in human urological tumor tissues. *Urol Res* 1998;26:395–9.
- Lebret T, Watson RW, Molin V, et al. Heat shock proteins Hsp27, Hsp60, Hsp70, and Hsp90: expression in bladder carcinoma. *Cancer* 2003;98:970–7.
- Ciocca DR, Oesterreich S, Chamness GC, McGuire WL, Fuqua SA. Biological and clinical implications of heat shock protein 27,000 (Hsp27): a review. *J Natl Cancer Inst* 1993;85:1558–70.
- Tomei LD, Kiecolt-Glaser JK, Kennedy S, Glaser R. Psychological stress and phorbol ester inhibition of radiation-induced apoptosis in human peripheral blood leukocytes. *Psychiatry Res* 1990;33:59–71.
- Levine AJ, Momand J, Finlay CA. The p53 tumour suppressor gene. *Nature* 1991;351:453–6.
- Bonkhoff H, Fixemer T, Hunsicker I, Remberger K. Estrogen receptor gene expression and its relation to the estrogen-inducible Hsp27 heat shock protein in hormone refractory prostate cancer. *Prostate* 2000;45:36–41.
- Bruey JM, Paul C, Fromentin A, et al. Differential regulation of Hsp27 oligomerization in tumor cells grown *in vitro* and *in vivo*. *Oncogene* 2000;19:4855–63.
- Chi KN, Eisenhauer E, Fazli L, et al. A phase I pharmacokinetic and pharmacodynamic study of OGX-011, a 2'-methoxyethyl antisense oligonucleotide to clusterin, in patients with localized prostate cancer. *J Natl Cancer Inst* 2005;97:1287–96.
- Rocchi P, So A, Kojima S, et al. Heat shock protein 27 increases after androgen ablation and plays a cytoprotective role in hormone-refractory prostate cancer. *Cancer Res* 2004;64:6595–602.
- July LV, Beraldi E, So A, et al. Nucleotide-based therapies targeting clusterin chemosensitize human lung adenocarcinoma cells both *in vitro* and *in vivo*. *Mol Cancer Ther* 2004;3:223–32.
- Grossman HB, Wedemeyer G, Ren L, Wilson GN, Cox B. Improved growth of human urothelial carcinoma cell cultures. *J Urol* 1986;136:953–9.
- Kiyama S, Morrison K, Zellweger T, et al. Castration-induced increases in insulin-like growth factor-binding protein 2 promotes proliferation of androgen-independent human prostate LNCaP tumors. *Cancer Res* 2003;63:3575–84.
- Yu RZ, Geary RS, Monteith DK, et al. Tissue disposition of 2'-O-(2-methoxy) ethyl modified antisense oligonucleotides in monkeys. *J Pharm Sci* 2004;93:48–59.
- Miyake H, Yamanaka K, Muramaki M, Hara I, Gleave ME. Therapeutic efficacy of adenoviral-mediated p53 gene transfer is synergistically enhanced by combined use of antisense oligodeoxynucleotide targeting clusterin gene in a human bladder cancer model. *Neoplasia* 2005;7:171–9.
- Zellweger T, Miyake H, July LV, Akbari M, Kiyama S, Gleave ME. Chemosensitization of human renal cell cancer using antisense oligonucleotides targeting the antiapoptotic gene clusterin. *Neoplasia* 2001;3:360–7.
- Gleave M, Tolcher A, Miyake H, et al. Progression to androgen independence is delayed by adjuvant treatment with antisense Bcl-2 oligodeoxynucleotides after castration in the LNCaP prostate tumor model. *Clin Cancer Res* 1999;5:2891–8.
- Concannon CG, Orrenius S, Samali A. Hsp27 inhibits cytochrome *c*-mediated caspase activation by sequestering both pro-caspase-3 and cytochrome *c*. *Gene Expr* 2001;9:195–201.
- Mosser DD, Morimoto RI. Molecular chaperones and the stress of oncogenesis. *Oncogene* 2004;23:2907–18.
- Neckers L, Schulte TW, Mimnaugh E. Geldanamycin as a potential anti-cancer agent: its molecular target and biochemical activity. *Invest New Drugs* 1999;17:361–73.
- Miyake H, Nelson C, Rennie PS, Gleave ME. Acquisition of chemoresistant phenotype by overexpression of the antiapoptotic gene testosterone-repressed prostate message-2 in prostate cancer xenograft models. *Cancer Res* 2000;60:2547–54.
- Miyake H, Chi KN, Gleave ME. Antisense TRPM-2 oligodeoxynucleotides chemosensitize human androgen-independent PC-3 prostate cancer cells both *in vitro* and *in vivo*. *Clin Cancer Res* 2000;6:1655–63.
- Bruey JM, Ducasse C, Bonniaud P, et al. Hsp27 negatively regulates cell death by interacting with cytochrome *c*. *Nat Cell Biol* 2000;2:645–52.
- Charette SJ, Landry J. The interaction of Hsp27 with Daxx identifies a potential regulatory role of Hsp27 in Fas-induced apoptosis. *Ann N Y Acad Sci* 2000;926:126–31.
- Wytttenbach A, Sauvageot O, Carmichael J, Diaz-Latoud C, Arrigo AP, Rubinsztein DC. Heat shock protein 27 prevents cellular polyglutamine toxicity and suppresses the increase of reactive oxygen species caused by huntingtin. *Hum Mol Genet* 2002;11:1137–51.
- Guay J, Lambert H, Gingras-Breton G, Lavoie JN, Huot J, Landry J. Regulation of actin filament dynamics by p38 map kinase-mediated phosphorylation of heat shock protein 27. *J Cell Sci* 1997;110:357–68.
- Rane MJ, Pan Y, Singh S, et al. Heat shock protein 27 controls apoptosis by regulating AKT activation. *J Biol Chem* 2003;278:27828–35.

308 **OGX-427 Down-regulation of Hsp27 in Bladder Cancer**

36. Parcellier A, Schmitt E, Gurbuxani S, et al. Hsp27 is a ubiquitin-binding protein involved in I- κ B α proteasomal degradation. *Mol Cell Biol* 2003;23:5790–802.
37. Rocchi P, Beraldi E, Ettinger S, et al. Increased Hsp27 after androgen ablation facilitates androgen-independent progression in prostate cancer via signal transducers and activators of transcription 3-mediated suppression of apoptosis. *Cancer Res* 2005;65:11083–93.
38. Oesterreich S, Hilsenbeck SG, Ciocca DR, et al. The small heat shock protein Hsp27 is not an independent prognostic marker in axillary lymph node-negative breast cancer patients. *Clin Cancer Res* 1996;2:1199–206.
39. Somji S, Garrett SG, Sens DA, Sens MA. Heat shock protein 27 expression in human bladder. *Urol Pathol* 1998;9:1–15.
40. Rossi MR, Somji S, Garrett SH, Sens MA, Nath J, Sens DA. Expression of hsp 27, hsp 60, hsc 70, and hsp 70 stress response genes in cultured human urothelial cells (UROtsa) exposed to lethal and sublethal concentrations of sodium arsenite. *Environ Health Perspect* 2002;110:1225–32.
41. Kassem H, Sangar V, Cowan R, Clarke N, Margison GP. A potential role of heat shock proteins and nicotinamide *N*-methyl transferase in predicting response to radiation in bladder cancer. *Int J Cancer* 2002;101:454–60.
42. McGarvey TW, Meng RD, Johnson O, El-Deiry W, Malkowicz SB. Growth inhibitory effect of p21 and p53 containing adenoviruses on transitional cell carcinoma cell lines *in vitro* and *in vivo*. *Urol Oncol* 2001;6:155–62.
43. Miyake H, Hara I, Kamidono S, Gleave ME. Synergistic chemosensitization and inhibition of tumor growth and metastasis by the antisense oligodeoxynucleotide targeting clusterin gene in a human bladder cancer model. *Clin Cancer Res* 2001;7:4245–52.
44. Miyake H, Hanada N, Nakamura H, et al. Overexpression of Bcl-2 in bladder cancer cells inhibits apoptosis induced by cisplatin and adenoviral-mediated p53 gene transfer. *Oncogene* 1998;16:933–43.
45. Chang FL, Lai MD. The relationship between p53 status and anticancer drugs-induced apoptosis in nine human bladder cancer cell lines. *Anticancer Res* 2000;20:351–5.
46. Gleave ME, Monia BP. Antisense therapy for cancer. *Nat Rev Cancer* 2005;5:468–79.
47. Duggan BJ, Gray S, Johnston SR, Williamson K, Miyaki H, Gleave M. The role of antisense oligonucleotides in the treatment of bladder cancer. *Urol Res* 2002;30:137–47.
48. Duggan BJ, Cotter FE, Kelly JD, et al. Antisense Bcl-2 oligonucleotide uptake in human transitional cell carcinoma. *Eur Urol* 2001;40:685–95.
49. Aiello LP, Brucker AJ, Chang S, et al. Evolving guidelines for intravitreal injections. *Retina* 2004;24:S3–19.

Molecular Cancer Therapeutics

Hsp27 knockdown using nucleotide-based therapies inhibit tumor growth and enhance chemotherapy in human bladder cancer cells

Masayuki Kamada, Alan So, Mototsugu Muramaki, et al.

Mol Cancer Ther 2007;6:299-308. Published OnlineFirst January 11, 2007.

Updated version Access the most recent version of this article at:
doi:[10.1158/1535-7163.MCT-06-0417](https://doi.org/10.1158/1535-7163.MCT-06-0417)

Cited articles This article cites 47 articles, 14 of which you can access for free at:
<http://mct.aacrjournals.org/content/6/1/299.full#ref-list-1>

Citing articles This article has been cited by 18 HighWire-hosted articles. Access the articles at:
<http://mct.aacrjournals.org/content/6/1/299.full#related-urls>

E-mail alerts [Sign up to receive free email-alerts](#) related to this article or journal.

Reprints and Subscriptions To order reprints of this article or to subscribe to the journal, contact the AACR Publications Department at pubs@aacr.org.

Permissions To request permission to re-use all or part of this article, use this link
<http://mct.aacrjournals.org/content/6/1/299>.
Click on "Request Permissions" which will take you to the Copyright Clearance Center's (CCC) Rightslink site.